PCCP

ROYAL SOCIETY OF CHEMISTRY

PAPER

View Article Online
View Journal | View Issue

Cite this: *Phys. Chem. Chem. Phys.*, 2020, **22**, 10212

Halogen bonding matters: visible light-induced photoredox catalyst-free aryl radical formation and its applications†

Rong Miao,[a] Dan Wang,[a] Jianliang Xiao,[a] Jiani Ma,[b] Dong Xue,*[a] Fengyi Liu *[a] and Yu Fang *[a]

Received 20th February 2020,
Accepted 20th April 2020

DOI: 10.1039/d0cp00946f

rsc.li/pccp

Photo-involving aryl halide activation plays a pivotal role in organic synthesis and materials science. Revealing the mechanism and understanding the photophysical and photochemical processes in the activation is of great importance. Here, we found that aryl halides could be directly activated to form aryl radicals *via* halogen bonding under visible light irradiation without using photocatalysts or high power light. The interaction between the aryl halide and Lewis base (Et_3N), as well as the triplet state formation, play crucial roles. Halogen bonding between aryl halide and Et_3N facilitates intersystem crossing (ISC) and leads to an abundance of the triplet aryl halide/Et_3N complex, where the carbon–halogen bond is much lengthened and prone to fracture. Therefore, visible light-driven photoredox catalyst-free C–C coupling reaction and radical-initiated polymerization were achieved. Avoiding the use of a catalyst not only brings convenience for low-cost operation, but also facilitates further purification. Meanwhile, the wide scope of aryl halide tolerance provides opportunities for chemical synthesis and polymerization.

1. Introduction

Studying the underlying photochemical process and developing a feasible method for visible-light-driven synthesis is an important area in the field of chemistry. Accurate understanding of a reaction is not only helpful for new system designs but also beneficial for process optimization in related research fields. Aryl halides, one of the most frequently used reactants in transition metal catalyzed C–C bond-forming reactions, are also favorable candidates for light-driven synthesis.[1–4] With rapid developments in photochemistry, remarkable progress has been achieved in aryl halide-based photosynthesis.[5–7] In the early years, aryl halides were usually activated under high power UV light *via* a hemolytic process or a radical anion-mediated process, where the aryl halide changed into an aryl halide radical anion when it received an electron from a Lewis base.[8,9] In recent years, visible light-driven aryl halide activation has been reported in which a photoredox catalyst is indispensable.[10,11] It is proposed that electron transfer happens between the excited photoredox catalyst and a base; and the formed ionic complex (usually the photoredox catalyst radical anion) then serves as the reductive species to react with the aryl halide to produce the aryl halide radical anion (top left in Scheme 1).[10–12] Arising from heat-induced base-promoted homolytic aromatic substitution (BHAS), BHAS has also been realized in visible light-induced aryl halide activation with the help of KO^{t}Bu (in DMSO).[13,14] So far, an acknowledged explanation for BHAS reactions is that the dimsyl anion from DMSO is the key ingredient, which further reacts with aryl halides *via* single electron transfer (SET) to produce the aryl halide radical anion (top right in Scheme 1).[15] Though there are many differences between these methods in terms of reaction conditions, the Lewis base is

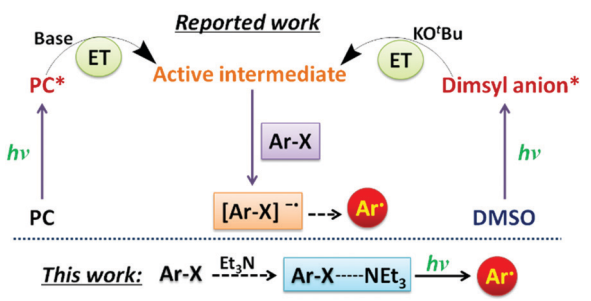

Scheme 1 Comparison of different mechanisms for aryl halide activation. PC: photoredox catalyst; Ar-X: aryl halide; ET: electron transfer.

[a] *Key Laboratory of Applied Surface and Colloid Chemistry, Ministry of Education, School of Chemistry and Chemical Engineering, Shaanxi Normal University, Xi'an 710062, People's Republic of China. E-mail: yfang@snnu.edu.cn*
[b] *College of Chemistry and Materials Science, Northwest University, Xi'an 710127, People's Republic of China*

† Electronic supplementary information (ESI) available. See DOI: 10.1039/d0cp00946f

indispensable and the formation of an aryl halide radical anion is a crucial step in all cases (top side of Scheme 1).

Intermolecular halogen bonding, which often occurs between electron-deficient halogen substituents and halogen bond acceptor atoms such as nitrogen, is an electrostatically driven, noncovalent interaction.[16,17] It is well recognized as an important interaction in biological systems, supramolecular chemistry, and molecular crystals.[18–20] Crucially, halogen bonding is also an effective strategy to control the spin state and reactivity of some species, such as aryl halides and carbenes.[21,22] However, to the best of our knowledge, the role of halogen bonding in aryl halide activation remains unexplored.

Herein, we demonstrate that halogen bonding is of great importance in aryl halide activation. Theoretical calculations reveal that the structure of the halogen bonding complex (aryl halide/Et_3N) changes a lot when it is excited into the triplet state *via* intersystem crossing. In the triplet state, the carbon–halogen bond in a halogen bonding complex is prone to breaking. Thus, an aryl halide can be directly activated under visible light in the presence of a Lewis base (downside of Scheme 1). Moreover, the activated aryl halides can be used in both C–C coupling reaction and radical initiated polymerization under mild conditions, where only an appropriate amount of Et_3N is needed and neither a photoredox catalyst nor a strong base is required. It is expected that the proposed mechanism as well as the presented reactions will facilitate further studies in related areas.

2. Experimental and computation methods

The reaction was carried out in a homemade photochemical reactor (Fig. S1, ESI†) with a 400 nm LED (Fig. S2, ESI†). In a typical experiment, a 5 mL glass vial was charged with acetonitrile (2 mL) and 4′-iodoacetophenone (4-I-COMe, 0.1 mmol). The solution was degassed *via* a syringe needle for 20 min, and Et_3N (30 μL) was added during the process. *N*-Methylpyrrole (2.4 mmol, 24 equiv.) was added to the deoxygenized mixture and the vial was sealed up and the reaction mixture was irradiated through the bottom side of the vial using a homemade reactor with an LED light of 400 nm for 12 h. The reaction was monitored using thin-layer chromatography (TLC) analysis. When the reaction is completed, the reaction mixture was transferred into a 25 mL round-bottom flask and then concentrated in a vacuum at 30 °C. Purification of the crude product was achieved by column chromatography using petrol ether/ethyl acetate (v/v = 10 : 1) on a silica gel column. The isolated compounds were characterized by high resolution ESI as well as ^1H and ^{13}C NMR spectroscopies.

The geometrical optimizations were done at the M062X-D3 level of theory with a def2-SVPD basis set and SMD solvation model using acetonitrile as the solvent (ε = 35.69). The time-dependent (TD) density functional was used for the S_1 state. The MS-CASPT2 singlet-point calculations coupled with the RASSI(SO) algorithm was carried out on top of the DFT-optimized PECs in order to obtain corrected energies as well as to evaluate the spin–orbit coupling effects.

3. Results and discussion

Referring to the reported work, it is speculated that there would be halogen bonding between aryl halide and Et_3N.[23,24] The ^{14}N NMR technique was used to study the interaction between aryl halide and Et_3N (Fig. 1). 2-Chlorobenzonitrile was chosen for the ^{14}N NMR study, as the N atom in the –CN group would be used as a reference for chemical shift comparison. Compared with the ^{14}N NMR spectrum of individual 2-chlorobenzonitrile or Et_3N, the peak around 1 ppm belongs to the N atom from Et_3N; the peak around 225 ppm belongs to the N atom in the –CN of 2-chlorobenzonitrile.[25] It is noted that the N atom form of Et_3N shifted to a lower field in the mixture (2-chlorobenzonitrile and Et_3N), while no obvious change was found for the N atom in the –CN group. Based on the ^{14}N NMR results, it is reasonable to conclude that there must be an interaction between the halogen atom in the aryl halide and the N atom in Et_3N, which is the expected halogen bonding.

3.1 Theoretical calculations

Halogen bonding between aryl halide and Et_3N was also confirmed using theoretical calculations. To study the interaction between aryl halide and Et_3N, 4-I-COMe and 4-Cl-COMe were used. Similar results were obtained for both the aryl halides tested. When Et_3N is introduced, the aryl halide and the Lewis base were loosely combined as a complex (S_0-min) by a halogen bond formed between I/Cl and N atoms (left part in Fig. 2A).[26–28]

The excited complexes are crucial for a light-induced synthesis, as they are key intermediates in the photochemical reaction. Therefore, the structure of the halogen bonding complex (aryl halide/Et_3N) in the excited state was optimized and studied. Multireference *ab initio* calculations were done and the results showed that the excited aryl halide existed in both singlet (S_1) and triplet states (T_1). Compared with the ground state, the structure of the complex changed little when they were in S_1; however, the structure of the complex changed a lot when they

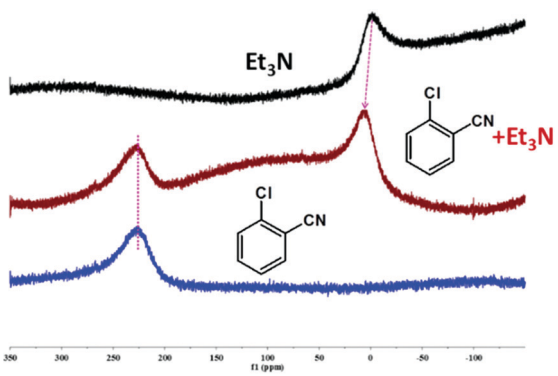

Fig. 1 ^{14}N NMR spectra of 2-chlorobenzonitrile (blue trace), Et_3N (black trace) and the mixture (red trace). Solvent: DMSO-d_6. Concentration of 2-chlorobenzonitrile was 0.1 M and 2 equiv. Et_3N was added.

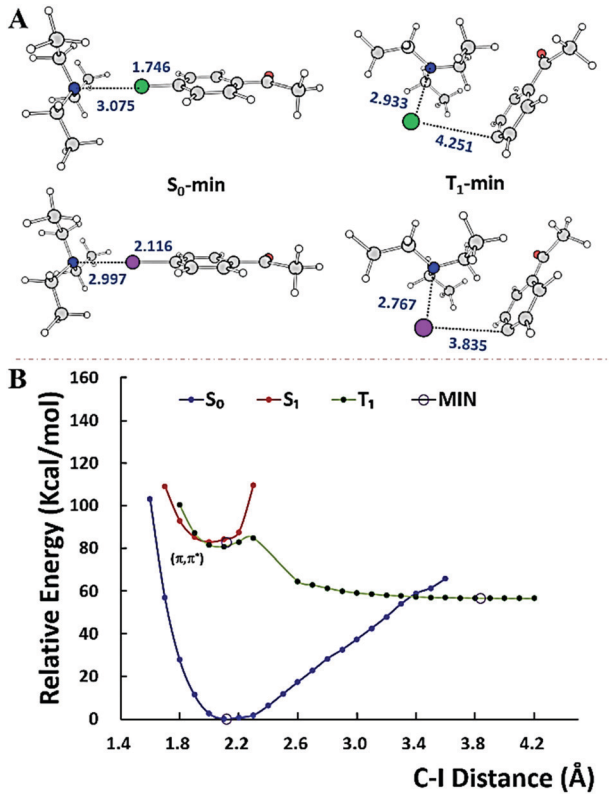

Fig. 2 Theoretical study on the halogen complex of aryl halide and Et_3N. (A) Structures of S_0 and T_1 minima of halogen bonding complexes (gray: carbon, white: hydrogen, green: chloride, purple: iodine); 4-Cl-COMe/Et_3N (top) and 4-I-COMe/Et_3N (down). (B) $S_1/T_1/S_0$ potential energy curves optimized at the (TD)M062X-D3/def2-SVPD(ECP) level with MS-CASPT2/ANO-RCC-VDZP energy corrections. The optimized minima on the MEPs are emphasized by the purple circles.

were in the triplet state. The most obvious difference is the extremely lengthened halogen bond compared with the singlet state (Fig. 2A), indicating a much weaker and more fragile carbon–halogen bond. The systematic calculation in Fig. S3 (ESI†) reveals that during the photo-cleavage of the C–I bonds in 4-I-COMe, the repulsive singlet and triplet $\pi\sigma^*$ excited states roughly decrease from the Franck–Condon region to a longer C–I distance. With the elongation of the C–I bond, the downhill $\pi\sigma^*$ states and uphill ground state become close in energy, which finally leads to a nearly degenerate situation at the dissociative structure (*i.e.*, $d_{C-I} > 4.0$ Å).

The interaction between aryl halide and Et_3N effectively tunes the electronic structure of 4-I-COMe and, as expected, alters the excited state PECs of C–I cleavage. Fig. 2B illustrates the optimized minima on S_0 and T_1 states as well as the PECs obtained at the MS-CASPT2//TD-M062X-D3 level of theory. On the T_1 PEC, a shallow minimum (T_1-min) emerges at a C···I distance of 3.835 Å.[29–31] The considerably elongated C···I distance and shortened I···N distance in T_1-min, with respect to those in S_0-min, suggest that the T_1-min is composed of two different fragments (Et_3NI···aryl group) from S_0-min. Natural bonding orbitals (NBO) charge distribution analyses further confirm a homolytic pattern of C–I bond cleavage. Thus, in the presence of Et_3N, the photo-induced cleavage of 4-I-COMe generates an aryl radical that is protected by a loosely bonded Et_3N···I moiety, suggesting that the intersystem crossing (ISC) between S_1 and T_1 is efficient. Spin–orbit treatments at the MS-CASPT2/RASSI-SO level showed that the S_1 and T_1 states indeed have a large magnitude of spin–orbit interaction matrix elements, and the spin orbit coupling (SOC) S_1 state has a significant contribution from spin-free T_1 in the range of 2.6–3.0 Å.[32,33] Both suggest an efficient $S_1 \rightarrow T_1$ ISC process. More detailed discussion and supplementary data (Fig. S3–S7 and Table S1) on theoretical calculations are provided in the ESI.†

Overall, theoretical calculations reveal that the carbon–halogen bond probably undergoes cleavage through the triplet state, which is in accordance with the well-known heavy atom effect. Meanwhile, theoretical calculations suggest that the Lewis base (Et_3N) not only plays a role in photo-activation of the C–I bond, but also serves as a protection group to stabilize the metastable aryl radical, which indicates the crucial role of halogen bonding in the activation process.

3.2 Photophysical study

To verify the validity of the results from theoretical calculations, experimental studies were carried out. 4-I-COMe was chosen as a model molecule, as it showed superior photophysical properties, which would facilitate further mechanistic study. First, fluorescence and phosphorescence behaviors of the 4-I-COMe before and after addition of Et_3N were investigated (Fig. 3). To ensure reliable intensity comparison, all the parameters were kept the same during the whole measurement.

Both fluorescence (Fig. 3A) and phosphorescence (Fig. 3B and Fig. S8, ESI†) of 4-I-COMe were enhanced after the addition of Et_3N, which is in accordance with the results from solid state studies.[34] Meanwhile, the maximum emission wavelength of phosphorescence showed an obvious blue shift (inset picture of Fig. 3B) and the phosphorescence lifetime of 4-I-COMe increased after Et_3N addition (Fig. S8, ESI†). These results

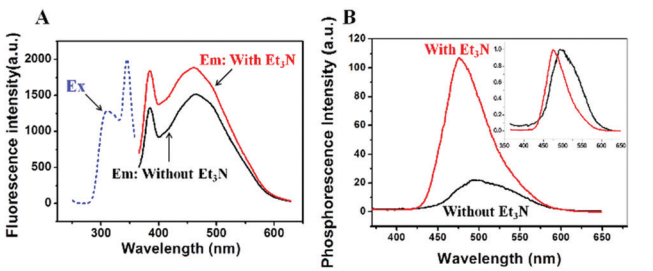

Fig. 3 Luminescence behavior of 4-I-COMe in the absence/presence of Et_3N. (A) Fluorescence spectra of 4-I-COMe in the absence (black) and in the presence (red) of Et_3N (λ_{ex} = 360 nm). The dashed blue line is the excitation spectrum. (B) Phosphorescence spectra of 4-I-COMe in the absence (black) and in the presence (red) of Et_3N (λ_{ex} = 360 nm). The inset picture shows the normalized phosphorescence spectra of B. The concentration of 4-I-COMe was 0.1 M and 2 equiv. Et_3N was added. The fluorescence spectrum was recorded at room temperature (25 °C), but the phosphorescence measurements were done by freezing the 4-I-COMe solution under liquid nitrogen for 5 min.

confirmed the interaction, probably halogen bonding, between 4-I-COMe and Et_3N. It is worth mentioning that the phosphorescence of 4-I-COMe increased nearly 10 times after interacting with Et_3N (Fig. 3B), suggesting that the halogen bonding complex (4-I-COMe/Et_3N) had higher ISC efficiency than 4-I-COMe.

In addition, the nanosecond transient absorption (Ns-TA) technique was used to study triplet absorption of 4-I-COMe without or with Et_3N (Fig. S9, ESI†). It was observed that the spectra of the 4-I-COMe/Et_3N complex showed higher OD values than that of 4-I-COMe under the same concentration, implying a higher triplet species ratio in the complex. Both Ns-TA spectra of the complex and 4-I-COMe showed negative absorption around 469 nm, which should arise from the fluorescence emission of the system (*cf.* Fig. 3A). Existence of the aryl halide in the triplet state was also verified by using 4-I-COMe as a triplet photosensitizer. A commonly used singlet oxygen ($^1O_2$) scavenger, 1,5-dihydroxyl naphthalene (DHN), was chosen. Upon irradiation under visible light (400 nm LED), characteristic absorption of DHN at 301 nm decreased and a new peak at 427 nm belonging to juglone appeared, which is due to oxidation of DHN by $^1O_2$ (Fig. S10a, ESI†).[35,36] Addition of 4-I-COMe in DHN solution could accelerate the oxidation process (Fig. S10b, ESI†), implying that 4-I-COMe can be used as a triplet sensitizer. In the control experiment, no juglone was found in the dark, suggesting light is indispensable. All these photophysical study results provided solid proof not only for the interaction between 4-I-COMe and Et_3N but also for the suggestion that halogen bonding would facilitate the ISC process. Combined with theoretical calculations, it is rational to speculate that the aryl radical would be obtained directly *via* halogen bonding-facilitated triplet state rupture under light irradiation.

3.3 Application of the activated aryl halide radical

To testify the speculation of the halogen bonding-facilitated direct aryl radical formation mechanism, 2,2,6,6-tetramethyl piperidinoxyl (TEMPO) was used as a trapping agent for the aryl radical. As expected, the TEMPO-trapped aryl radical was found when TEMPO was added into the mixture of 4-I-COMe and Et_3N under visible light irradiation (Fig. S11, ESI†). Meanwhile, an abundance of the dehalogenation product (acetophenone) was obtained after the mixture of 4-I-COMe and Et_3N was irradiated for 12 h (Fig. S12, ESI†), while little acetophenone was found in the reaction without Et_3N. These results certified the formation of the aryl radical and provide solid proof for the proposed halogen bonding activation process deduced from theoretical calculations and experimental results. What's more, success in aryl radical acquisition paves the way for further application, as aryl radicals are highly reactive species and they are important intermediates in organic synthesis and materials science.

3.3.1 Visible light-driven C–C coupling reaction. Based on the revealed mechanism, the light-induced photoredox catalyst-free C–C coupling reaction was explored by choosing 4-iodoacetophone (4-I-COMe) and a well-known trapping agent, *N*-methylpyrrole (Scheme 2).[12,37,38] An appropriate amount of Et_3N was introduced and the reactions were done under light of

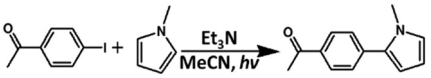

Scheme 2 The model reaction in this work.

different wavelengths (LED, 365 nm, 400 nm, 465 nm, 520 nm and white light). As is shown in Table 1, C–C coupling products were obtained for most tests. It is worth noting that excellent yields (99%) were obtained for 400 nm light irradiation.

Except for the green light (LED, wavelength of 520 nm), all the lights used with different wavelengths are capable to induce the reaction, though the coupling yields are different (entries 1–5, Table 1). After 12 hours of reaction, the UV light (LED, 365 nm) irradiation gave a yield of 84%, the purple light (LED, 400 nm) gave a yield of 99%, the blue light (LED, 465 nm) gave a yield of 54% and the white light led to a yield of 19%, which demonstrates that purple light (Table 1) irradiation is more efficient than others. Therefore, 400 nm LED light was chosen as the preferable light source in further studies.

The control experiment was carried out without light and no product was found (entry 6, Table 1), which reveals that light irradiation is necessary for the reaction. Although similar reactions have been carried out by König *et al.*, photoredox catalysts (organic fluorophores) must be used in their systems. However, benefiting from the re-understanding of the photophysical and photochemical processes, no photoredox catalyst is needed in the as-reported work. To further test the reliability of the proposed mechanism, control experiments were done and different reactions were conducted under varied conditions. First, the effect of the base was investigated and no product was found without a base, indicating the crucial role of the interaction between aryl halide and the base (entry 6, Table S2, ESI†). In addition, the amount of base also matters, sufficient base is needed but too much base is not advisable (entries 5, 7, 8, Table S2, ESI†). These results indicate that the base is indispensable for the reaction indicating the crucial role of halogen bonding in the reaction.

Second, different solvents were chosen and it turned out that polar solvents, such as MeCN and DMF, are more favorable for the reaction (Table S3, ESI†), which is similar to some reported work.[12] Third, the amount of *N*-methylpyrrole was also varied and it showed that coupling yield increased when the concentration of *N*-methylpyrrole increased (entries 1–5, Table S4, ESI†).

Table 1 Photoredox catalyst-free C–C coupling reaction under different lights

Entry	Light	Yield (%)
1	365 nm	80
2	400 nm	99
3	465 nm	54
4	520 nm	0
5	White light	19

Reaction time: 12 h; 2 equiv. Et_3N; and the yields were determined by ^1H NMR analysis of the crude reaction mixture with the standard after the reaction.

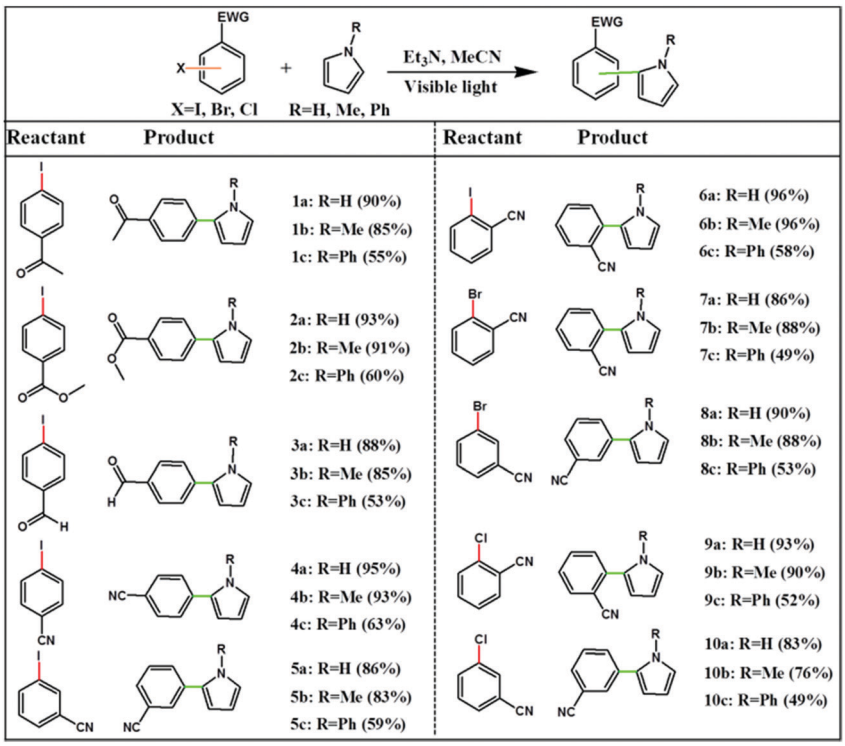

Fig. 4 Substrate scope for photoredox catalyst-free C–C coupling reaction. Reaction conditions are the same as in Table 1, entry 2 except for *N*-phenylpyrrole derivatives, where 4 equiv. of *N*-phenylpyrrole was used.

The coupling yield reached the highest value when 24 equivalents of *N*-methyl pyrrole were used (entry 4, Table S4, ESI†), which is similar to the reported work where excess *N*-methylpyrrole was used.[38,39] In addition, it was found that deoxygenization is helpful for the reaction and the yield was lower when the reaction was done with air (closed system without deoxygenization), which infers that there must be oxygen-sensitive intermediates in the reaction system. All these control experiments show that light and base are indispensable in the reaction, which implies the importance of halogen bonding and ISC and further confirms the proposed mechanism. Subsequently, the scope of the reaction was examined by choosing different aryl halides and pyrroles (Fig. 4). Not only aryl iodides, but also aryl bromides and chlorides are allowed with excellent yields. It was found that the method is more suitable for aryl halides with electron withdrawing groups, such as COOMe, COMe, CHO and CN. The corresponding arylation products were obtained in good to excellent yields when the three pyrrole derivatives (N–H, N–Me, N–Ph) were used, suggesting good tolerance of the reaction.

3.3.2 Visible light-driven polymerization. According to the interesting findings, an attempt was made to use the reported system in light-induced polymerization, which was considered a revolution in polymer science.[40,41] Different from the reported work for light-induced polymerization,[42,43] where only limited initiators (such as 2-cyanopropyl iodide) were used, we found that an abundance of aryl halides with electron withdrawing groups could serve as initiators in the presence of Et_3N.

Table 2 Photoredox catalyst-free light-induced polymerization

Aryl halide	Monomer	Con. (%)	*t* (h)	M_n	PDI
4-I-COMe	MMA	85	3	76 702	2.32
4-I-CN	MMA	82	3	47 954	1.84
4-I-COMe	BuAC	89	2	26 314	1.75
4-Br-COMe	BuAC	78	2	47 803	1.92
4-Cl-COMe	BuAC	72	2	91 574	1.80
2-I-CN	BuAC	94	2	56 193	2.01

Aryl halide: 0.1 mmol (1 equiv.); monomer: 100 equiv.; Et_3N: 2 equiv.; MMA: methyl methacrylate; BuAC: butyl acrylate. M_n and PDI was determined by gel permeation chromatography (GPC) with a multiangle laser light-scattering (MALLS) detector.

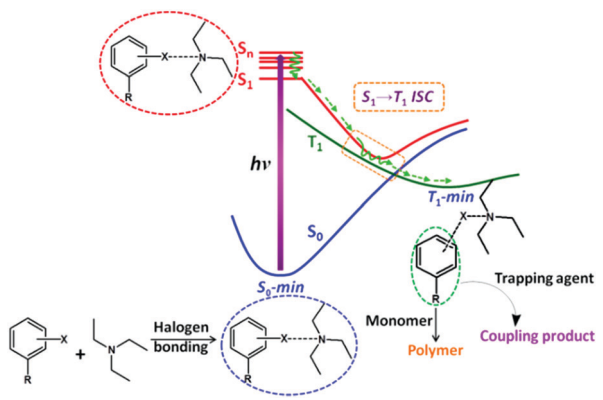

Scheme 3 Proposed reaction mechanism for catalyst-free visible-light-driven reaction.

Meanwhile, it was noticed that molecular weight of the obtained polymers goes in the order of iodo- < bromo- < chloro- when aryl halides with the same EWG was used as initiators, which indicates that molecular weights of the polymers can be easily tuned by halogen substitution (Table 2).

Clearly, all the results from the reaction study are in accordance with the presented mechanism. Therefore, a plausible mechanism is illustrated in Scheme 3 to give a clear image of the reaction process.

4. Conclusions

Though the deep understanding of a reaction mechanism is a great challenge, especially for photo-induced reactions, we would benefit a lot when we have a clear image of the reaction process. We tried to involve halogen bonding in understanding the photophysical and photochemical processes in aryl halide activation. Both experimental studies and theoretical calculations reveal that halogen bonding plays a crucial role in the process. Different from the reported mechanisms, where aryl halide radical anion is the key intermediate, we found that the carbon–halogen bond in a halogen bonding complex can be directly decomposed under visible light irradiation. The halogen bonding complex can be easily excited to the triplet state *via* intersystem crossing, where the carbon–halogen bond is highly activated for rupture. Based on these findings, we have successfully demonstrated photoredox catalyst-free visible-light-driven aryl halide activation for C–C coupling reactions and radical initiated polymerization. Avoiding the use of a catalyst not only brings convenience for low-cost operation, but also facilitates further purification and brings in excellent coupling yields. Meanwhile, the wide scope of aryl halide tolerance provides plenty of opportunities for radical initiated polymerization, which would contribute to functionalization of polymers and thus facilitate further applications. We anticipate that the revealed photophysical and photochemical process for aryl halide activation as well as the reactions will provide new strategies and opportunities in organic chemistry, materials science and photochemistry.

Conflicts of interest

There are no conflicts to declare.

Acknowledgements

We acknowledge funding from the Natural Science Foundation of China (21603139, 21527802, 21673133, 21820102005), the 111 project (B14041), the China Postdoctoral Science Foundation (1202040102), and the Program for Changjiang Scholars and Innovative Research Team in University (IRT-14R33). The authors also thank Gang Li and Liu Yang *et al.* for duplication experiments to verify the reaction yields.

Notes and references

1 M. Silvil, C. Verrier, Y. Rey, L. Buzzetti and P. Melchiorre, *Nat. Chem.*, 2017, **9**, 868.
2 H. Kim and C. Lee, *Angew. Chem., Int. Ed.*, 2012, **51**, 12303.
3 J. Grimshaw, *Chem. Soc. Rev.*, 1982, **13**, 185.
4 S. Protti, M. Fagnoni and A. Albini, *Angew. Chem., Int. Ed.*, 2005, **44**, 5675.
5 J. Yin and S. L. Buchwald, *Org. Lett.*, 2000, **2**, 1101.
6 M. Majek and A. J. V. Wangelin, *Acc. Chem. Res.*, 2016, **49**, 2316.
7 S. Zhou, G. M. Anderson, B. Mondal, E. Doni, V. Ironmonger, M. Kranz, T. Tuttle and J. A. Murphy, *Chem. Sci.*, 2014, **5**, 476.
8 J. Grimshaw, *Chem. Soc. Rev.*, 1981, **10**, 181.
9 C. Gall, *Chem. Rev.*, 1988, **88**, 765.
10 Z. Zuo, D. Ahneman, L. Chu, J. Terrett, A. G. Doyle and D. W. C. MacMillan, *Science*, 2014, **345**, 437.
11 I. Ghosh, L. Marzo, A. Das, R. Shaikh and B. König, *Acc. Chem. Res.*, 2016, **49**, 1566.
12 I. Ghosh, T. Ghosh, J. I. Bardagi and B. König, *Science*, 2014, **346**, 725.
13 M. E. Budén, J. F. Guastavino and R. A. Rossi, *Org. Lett.*, 2013, **15**, 1174.
14 J. F. Guastavino, M. E. Budén and R. A. Rossi, *J. Org. Chem.*, 2014, **79**, 9104.
15 M. E. Budén, J. I. Bardagí, M. Puiatti and R. A. Rossi, *J. Org. Chem.*, 2017, **82**, 8325.
16 G. Cavallo, P. Metrangolo, R. Milani, T. Pilati, A. Priimagi, G. Resnati and G. Terraneo, *Chem. Rev.*, 2016, **116**, 2478.
17 F. Zordan, L. Brammer and P. Sherwood, *J. Am. Chem. Soc.*, 2005, **127**, 5979.
18 A. Priimagi, G. Cavallo, P. Metrangolo and G. Resnati, *Acc. Chem. Rev.*, 2013, **46**, 2686.
19 L. Meazza, J. Foster, K. Fucke, P. Metrangolo, G. Resnati and J. W. Steed, *Nat. Chem.*, 2013, **5**, 42.
20 L. Turunen, U. Warzok, R. Puttreddy, N. Beyeh, C. Schalley and K. Rissanen, *Angew. Chem., Int. Ed.*, 2016, **55**, 14033.
21 S. Henkel, P. Costa, L. Klute, P. Sokkar, M. Fernandez-Oliva, W. Thiel, E. Sanchez-Garcia and W. Sander, *J. Am. Chem. Soc.*, 2016, **138**, 1689.
22 D. Ravelli, S. Protti, M. Fagnoni and A. Albini, *J. Org. Chem.*, 2013, **48**, 3814.
23 M. Erdélyi, *Chem. Soc. Rev.*, 2012, **41**, 3547.
24 T. Shirman, R. Kaminker, D. Freeman and M. Boom,, *ACS Nano*, 2011, **5**, 6553.
25 D. Carnevale, X. Ji and G. Bodenhausen, *J. Chem. Phys.*, 2017, **147**, 184201.
26 J. Yang, X. Zhu, T. Wolf, Z. Li, J. Nunes, R. Coffee, J. Cryan, M. Gühr, K. Hegazy, T. Heinz, K. Jobe, R. Li, X. Shen, T. Veccione, S. Weathersby, K. Wilkin, C. Yoneda, Q. Zheng, T. Martinez, M. Centurion and X. Wang, *Science*, 2018, **361**, 64.
27 J. Neaton, *Science*, 2017, **358**, 167.
28 M. Langton, S. Robinson, I. Marques, V. Félix and P. Beer, *Nat. Chem.*, 2014, **6**, 1039.

29 J. Finley, P. Malmqvist and B. Roos, *Chem. Phys. Lett.*, 1998, **288**, 299.
30 Y. Zhao and D. Truhlar, *Theor. Chem. Acc.*, 2007, **120**, 215.
31 S. Grimme, *Wiley Interdiscip. Rev.: Comput. Mol. Sci.*, 2011, **1**, 211.
32 P. Malmqvist, B. Roos and B. Schimmelpfennig, *Chem. Phys. Lett.*, 2002, **357**, 230.
33 G. Karlström, R. Lindh, P. Å. Malmqvist, B. O. Roos, U. Ryde, V. Veryazov, P. O. Widmark, M. Cossi, B. Schimmelpfennig, P. Neograd y and L. Seijo, *Comput. Mater. Sci.*, 2003, **28**, 222.
34 H. Gao, Q. Shen, X. Zhao, X. Yan, X. Pang and W. Jin, *J. Mater. Chem.*, 2012, **22**, 5336.
35 N. Adarsh, M. Shanmugasundaram, R. R. Avirah and D. Ramaiah, *Chem. – Eur. J.*, 2012, **18**, 12655.
36 C. Zhang, J. Zhao, S. Wu, Z. Wang, W. Wu, J. Ma, S. Guo and L. Huang, *J. Am. Chem. Soc.*, 2013, **135**, 10566.
37 L. Zeng, T. Liu, C. He, D. Shi, F. Zhang and C. Duan, *J. Am. Chem. Soc.*, 2016, **138**, 3958.
38 I. Ghosh and B. König, *Angew. Chem., Int. Ed.*, 2016, **55**, 868.
39 I. Ghosh, R. S. Shaikh and B. König, *Angew. Chem., Int. Ed.*, 2017, **56**, 8544.
40 M. Chen, M. Zhong and J. A. Johnson, *Chem. Rev.*, 2016, **116**, 10167.
41 S. Shanmugam and C. Boyer, *Science*, 2016, **352**, 1053.
42 C. Wang and A. Goto, *J. Am. Chem. Soc.*, 2017, **139**, 10551.
43 L. Xiao, K. Sakakibara, Y. Tsujii and A. Goto, *Macromolecules*, 2017, **50**, 1882.

